IEEE Access
Multidisciplinary | Rapid Review | Open Access Journal

Received March 13, 2019, accepted March 30, 2019, date of publication April 4, 2019, date of current version June 12, 2019.

Digital Object Identifier 10.1109/ACCESS.2019.2908969

Dual-Band Eight-Antenna Array Design for MIMO Applications in 5G Mobile Terminals

JIANXING LI[1], (Member, IEEE), XIAOKE ZHANG[1], ZHI WANG[2], XIAOMING CHEN[1], (Senior Member, IEEE), JUAN CHEN[3], (Member, IEEE), YINGSONG LI[4], (Member, IEEE), AND ANXUE ZHANG[1]

[1]School of Electronic and Information Engineering, Xi'an Jiaotong University, Xi'an 710049, China
[2]School of Software Engineering, Xi'an Jiaotong University, Xi'an 710049, China
[3]Shenzhen Research School, Xi'an Jiaotong University, Shenzhen 518057, China
[4]College of Information and Communication Engineering, Harbin Engineering University, Harbin 150001, China

Corresponding author: Zhi Wang (zhiwang@xjtu.edu.cn)

This work was supported in part by the National Natural Science Foundation of China under Grant 61801369, in part by the China Postdoctoral Science Foundation under Grant 2018M631161, in part by the Natural Science Foundation of Shaanxi Province under Grant 2018JQ6081, in part by the Shaanxi Province Postdoctoral Science Foundation under Grant 2017BSHYDZZ14, in part by the Fundamental Research Funds for the Central Universities under Grant XJTU1191329860 and Grant HEUCFM180806, and in part by the Technology Program of Shenzhen under Grant JCYJ20170816100722642.

ABSTRACT This paper proposes a dual-band eight-antenna array for multiple-input and multiple-output (MIMO) applications in 5G mobile terminals. The designed MIMO antenna array comprises eight L-shaped slot antennas based on stepped impedance resonators (SIRs). The required dual-resonance can be obtained by adjusting the impedance ratio of the SIR, and good impedance matching can be ensured for each antenna element by tuning the position of the microstrip feed line. The experimental results show that a measured return loss of higher than 10 dB and a measured inter-element isolation of greater than 11.2 dB have been obtained for each antenna element with a simulated total efficiency of larger than 51% across the long term evolution (LTE) band 42 (3400–3600 MHz) and LTE band 46 (5150–5925 MHz). In addition, the measured envelope correlation coefficient (ECC) is lower than 0.1 between arbitrary two antenna elements, and the proposed MIMO antenna array realizes a simulated channel capacity of higher than 36.9 bps/Hz within both operation bands. Furthermore, the MIMO antenna array can maintain acceptable radiation and MIMO performance in the presence of specific anthropomorphic mannequin (SAM) head and human hands.

INDEX TERMS Channel capacity, dual-band, multiple input and multiple output (MIMO), slot antenna, stepped impedance resonator (SIR).

I. INTRODUCTION

Due to the tremendous prosperity of modern communication systems, people have been demanding more and more rapid information transmission rate. Consequently, it is essential to possess a much greater channel capacity for modern wireless communication systems, which promotes the development of 5G communications significantly. The world is to usher 5G communications in the near future. It is well known that the multiple input and multiple output (MIMO) systems relying on multi-antennas as one of the crucial technologies for 5G operation can improve the channel capacity and enhance the communication reliability. The 5G communications needs to support higher data transmission rate, shorter time delay, and larger channel capacity compared to the 4G communications. The 2×2 and 4×4 MIMO antenna arrays resultantly have gradually failed to meet the rigorous requirement. Therefore, many researches have been conducted on the 8×8 MIMO antenna array designs, which are targeted to be applied in 5G mobile terminals [1], [2].

The long term evolution (LTE) band 42 (3400–3600 MHz) has been licensed as one of the sub-6GHz bands. Thus, many MIMO antenna arrays at LTE band 42 have been designed. In [3], an 8-port MIMO antenna array as well as a 16-port one have been studied, while a 12×12 MIMO antenna array has been proposed in [4]. However, the MIMO antenna array operating merely at the LTE band 42 cannot fully satisfy the demand of the forthcoming 5G multiband communications. The LTE band 46 (5150–5925 MHz), though still unlicensed, is a potential and competitive spectrum to be utilized for 5G

The associate editor coordinating the review of this manuscript and approving it for publication was Yejun He.

TABLE 1. Optimal physical dimensions of each antenna element.

Parameters	L_1 (mm)	L_2 (mm)	L_3 (mm)	L_4 (mm)	L_5 (mm)	W_1 (mm)	W_2 (mm)	W_3 (mm)	R_1 (mm)	R_2 (mm)
Ant 1/Ant 4/Ant 5/Ant 8	9.6	5.2	10.0	5.5	15.0	1.5	2.7	1.8	0.6	0.4
Ant 2/Ant 3/Ant 6/ Ant 7	10.0	6.3	10.0	4.3	15.0	1.5	2.7	1.8	0.5	0.4

MIMO applications [5]. The multimode resonator, multi-stub loaded resonator, and stepped impedance resonator (SIR) are promising candidates to develop the MIMO antenna array in mobile terminals. Due to the limited space, it is challenging to arrange a large number of antenna elements in a modern commonly-sized smartphones whilst maintain good isolation and radiation efficiency.

Various techniques have been investigated in the literature to realize the multiband MIMO antenna array of 5G mobile terminals [6]–[12]. The majority of these designs are based on multimode resonators or combination of different structures. An 8-antenna MIMO array has been analyzed to operate at the LTE band 42 and LTE band 46 [6]. Two distinct radiators, namely slot antenna and monopole antenna, are responsible for different bands. A return loss of higher than 6 dB and an envelope correlation coefficient (ECC) of smaller than 0.15 have been obtained. Furthermore, it achieves a high channel capacity. However, the vertically-oriented antenna elements increase the thickness and fabrication complexity. In [7], a triple band MIMO antenna array comprising three individual radiators, including an inverted π-shaped antenna, a longer L-shaped slot antenna, and a shorter L-shaped slot antenna, has been proposed. Each band is obtained by a different number of corresponding radiators. A return loss of higher than 6 dB and an ECC of less than 0.15 have been achieved.

In this paper, an 8-antenna MIMO array is proposed which operates at the LTE band 42 and LTE band 46 for future 5G mobile terminals. The MIMO antenna array is composed of eight slot antenna elements based on SIRs excited by shorted microstrip feed lines printed on the top side of the substrate. The slot antenna elements are realized in the ground plane printed on the bottom side of the substrate. The proposed MIMO antenna array has been simulated and validated by the measurements of a fabricated prototype. Good agreement between the measurement and simulation results has been observed, showing that the MIMO antenna array achieves good return loss, isolation, ECC, total efficiency, and channel capacity. The effects of the display panel on the performance of the MIMO antenna array have also been studied. Besides, the ECC and total efficiency of the MIMO antenna array also have been simulated and analyzed using CST Studio Suite 2016, in the presence of one hand, two hands and specific anthropomorphic mannequin (SAM) head.

II. DUAL-BAND EIGHT-ANTENNA MIMO ARRAY DESIGN

The geometrical configuration of the proposed dual-band 8-antenna MIMO array is given in Figure 1. The whole system is mounted on a FR4 ($\varepsilon_r = 4.4$, $\tan\delta = 0.025$) substrate with

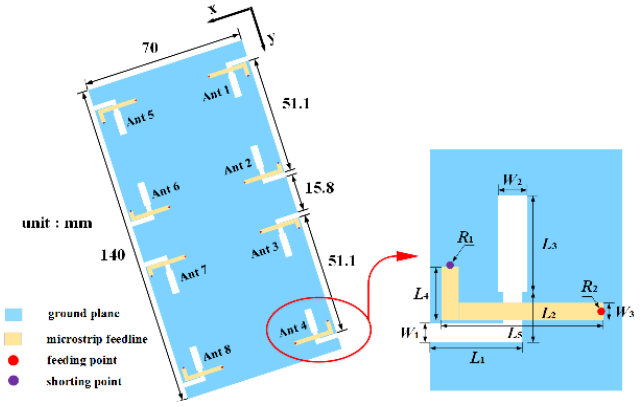

FIGURE 1. Geometrical configuration of the proposed 8-port dual-band MIMO antenna array.

a size of 140 mm × 70 mm × 1 mm. Each slot antenna element based on a SIR is excited by a 50 Ω microstrip line etched on the top side of the substrate. For each microstrip feed line, its one end is connected with a SMA connector and the other end is shorted to the ground to produce an inductance, and thus good impedance matching can be achieved.

According to [13], the multiband antenna can be attained by adjusting the impedance ratio and electrical length ratio of the SIR. With the purpose to obtain dual operation bands, the above two parameters need to be carefully selected. To simplify the calculation process and subsequent design, the electrical length ratio is assumed to be 1.0, the fundamental frequency is 3500 MHz, and the first harmonic frequency is 5500 MHz. Based on the above assumptions, the calculated impedance ratio is approximately 1.6. Hence, the slot lines with characteristic impedances of 40 Ω and 64 Ω, are used to accomplish the design. The lengths and positions of the microstrip feed lines can be adjusted, so that the designed MIMO antenna array can well operate in the required two frequency bands. Finally, the optimal physical dimensions for each antenna element are listed in Table 1.

III. SIMULATED RESULTS AND ANALYSIS

For the designed 8-port MIMO antenna array, the simulated *S*-parameters results and MIMO performance are presented in this section. Furthermore, the influences of the designed antenna array in the presence of user's hands and SAM head are also investigated and analyzed. Moreover, the effects of the display panel are also studied.

A. S-PARAMETERS AND EQUIVALENT SURFACE CURRENT DISTRIBUTIONS

The simulated *S*-parameters are shown in Figure 2. Note that only the simulated results of Ant 1 to Ant 4 are depicted due

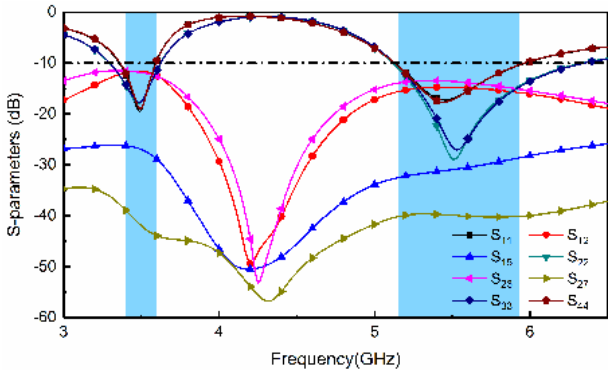

FIGURE 2. Simulated *S*-parameters of the MIMO antenna array.

to the symmetry of the designed MIMO antenna array. It can be obviously seen that the return loss of the designed 8-port MIMO antenna array are greater than 10 dB within the two frequency bands. Since the antenna elements along the same long side are close to each other, the mutual coupling, i.e. $S_{12}$and S_{23}, are relatively larger. However, the isolations are still greater than 11.8 dB which is acceptable. In comparison, the distances between the antenna elements on the same narrow side are further, and the mutual coupling, i.e. S_{15}, is therefore less than −25 dB across the two frequency bands. The mutual coupling between nonadjacent antenna elements are certainly rather weak.

To vividly illustrate the two resonant modes of the SIR-based slot antenna element, the simulated equivalent surface current distributions of Ant 1, respectively, at 3500 MHz and 5500 MHz are displayed in Figure 3. At 3500 MHz, it can be easily seen that the slot antenna operates at the fundamental quarter-wavelength resonant mode. In addition, two current nulls along the slot can be found when the antenna operates at 5500 MHz, i.e. the first harmonic resonant mode.

B. MIMO PERFORMANCE

The ECC defines the correlation level between the radiation patterns of any two antenna elements. It is the most important indicator to judge the performance such as diversity gain of a MIMO systems [14], [15]. The smaller the ECC is, the higher the diversity gain can be ensured. It is generally required that the ECC must be less than 0.5 to provide reasonable diversity gain [16].

The ECC between two antenna elements can be accurately calculated from their farfield radiation patterns using (1)

$$\rho_{ij} = \frac{\left| \iint_{4\pi} \overline{F}_i(\theta,\phi) \cdot \overline{F}_j^*(\theta,\phi)\, d\Omega \right|^2}{\iint_{4\pi} \left|\overline{F}_i(\theta,\phi)\right|^2 d\Omega \cdot \iint_{4\pi} \left|\overline{F}_j(\theta,\phi)\right|^2 d\Omega} \quad (1)$$

where ρ_{ij} denotes the ECC between element Ant i and Ant j, $\overline{F}_i(\theta,\phi)$ denotes the farfield radiation patterns of Ant i, and * denotes the Hermitian transpose of a matrix. Here, note that $\overline{F}_i(\theta,\phi)$ and $\overline{F}_j(\theta,\phi)$ are complex vectors. The ECC also

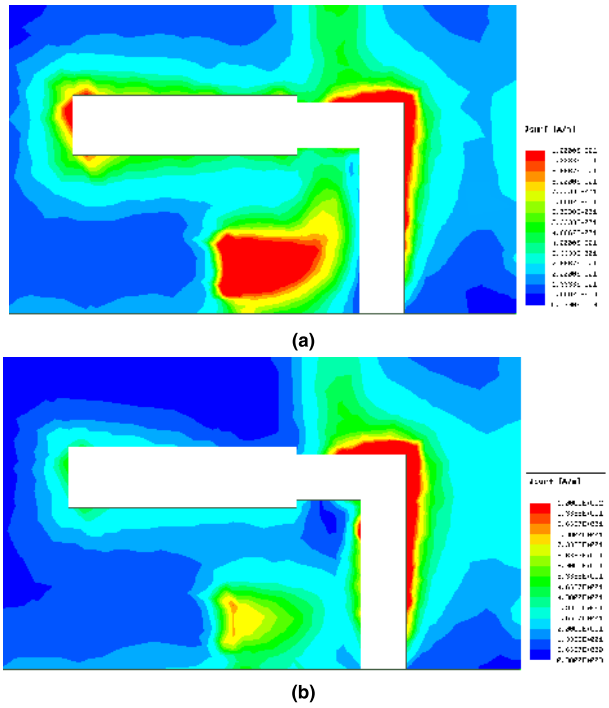

FIGURE 3. Simulated equivalent surface current distributions of Ant 1. (a) 3500 MHz. (b) 5500 MHz.

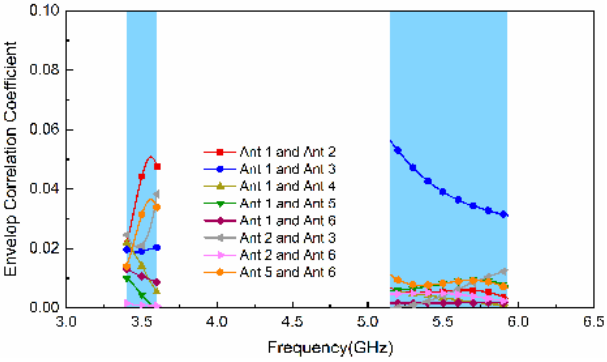

FIGURE 4. Simulated ECCs of the MIMO antenna array.

can be estimated from the *S*-parameters using (2)

$$\rho_{ij} = \frac{\left| S_{ii}^* S_{ij} + S_{ji}^* S_{jj} \right|^2}{\left(1 - \left(|S_{ii}|^2 + |S_{ji}|^2\right)\right)\left(1 - \left(|S_{jj}|^2 + |S_{ij}|^2\right)\right)} \quad (2)$$

where S_{ii} is the reflection coefficient of element Ant i, and S_{ij} $(i \neq j)$ is the transmission coefficient between element Ant i and element Ant j.

The simulated ECCs calculated from the farfield patterns are presented in Figure 4. Within both frequency bands, the ECCs between any two neighbor antennas are smaller than 0.1, while those between two nonadjacent antennas are even less than 0.02. It is sufficient to prove that any two antenna elements of the proposed MIMO antenna array have a mall correlation level within the two frequency bands.

The channel capacity means the maximum achievable data transmission rate [17], [18]. For a MIMO antenna array,

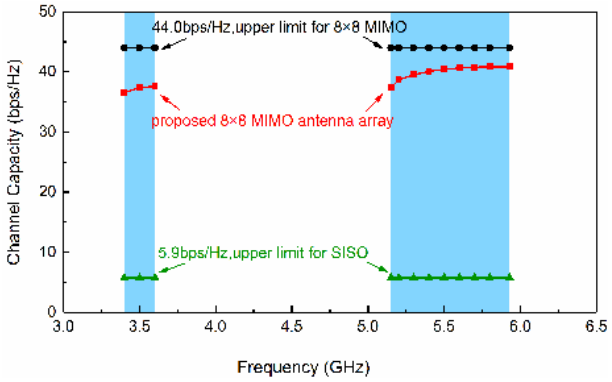

FIGURE 5. Simulated channel capacity when the SNR is 20 dB.

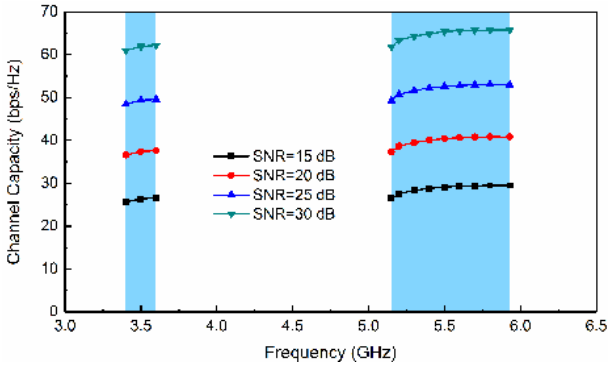

FIGURE 6. Simulated channel capacities with varying SNRs.

the larger the number of antenna elements is, normally the higher the channel capacity is. In general, the channel capacity of a MIMO antenna array can be calculated using (3) [19]

$$C = \log_2 \left[\det \left(I_N + \frac{SNR}{N} HH^* \right) \right] \tag{3}$$

where C is the channel capacity, SNR is the signal-to-noise ratio, N is the number of the antenna elements, I_N denotes a $N \times N$ identity matrix, and H is the matrix of the channel capacity.

The simulated channel capacity of the 8-antenna MIMO array is depicted in Figure 5. The communication channel is assumed to be an independently and identically distributed channel with the Rayleigh fading environment [6]. Given the SNR is 20 dB, by averaging 1,00,000 random Rayleigh fading channel realizations within the two frequency bands [7], the channel capacity of an ideal single input and single output (SISO) system is 5.9 bps/Hz, and that of an ideal 8×8 MIMO system should be 44 bps/Hz. The channel capacity of the proposed 8-antenna MIMO array is more than 36.9 bps/Hz across both operation bands, i.e. only 7.1 bps/Hz less than the theoretical upper bound. Within the LTE band 46, the channel capacity is higher than 38.5 bps/Hz with a maximum of 40.9 bps/Hz. Moreover, the channel capacities with varying SNRs are shown in Figure 6. While the SNR is increased by 5 dB, the channel capacity is enhanced by 11 bps/Hz approximately.

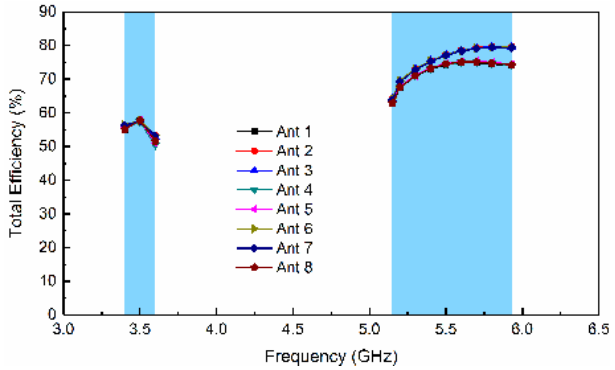

FIGURE 7. Simulated total efficiency of each antenna element.

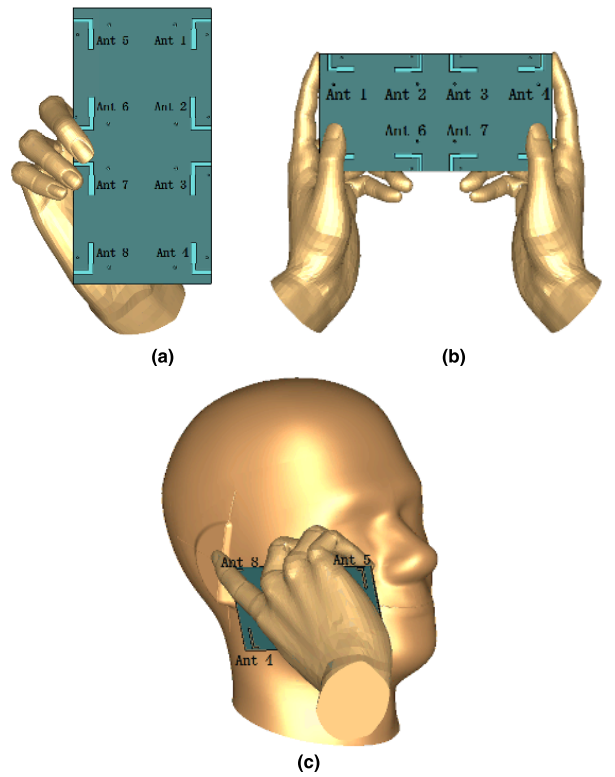

FIGURE 8. Three typical utility scenarios for mobile terminals. (a) Single hand. (b) Two hands. (c) SAM head and one hand.

C. TOTAL EFFICIENCY

The total efficiency of each antenna element of the proposed 8-antenna MIMO array is simulated and plotted in Figure 7. In the simulations, the matched 50 Ω loads are connected to other ports except the excited element. The total efficiencies are about from 51% to 59% and from 62% to 80% across the 3500-MHz band and 5500-MHz band, respectively.

D. EFFECTS OF SAM HEAD AND USER'S HANDS

Since the proposed 8-antenna MIMO array is to be utilized in 5G mobile terminals, the impacts of human head and

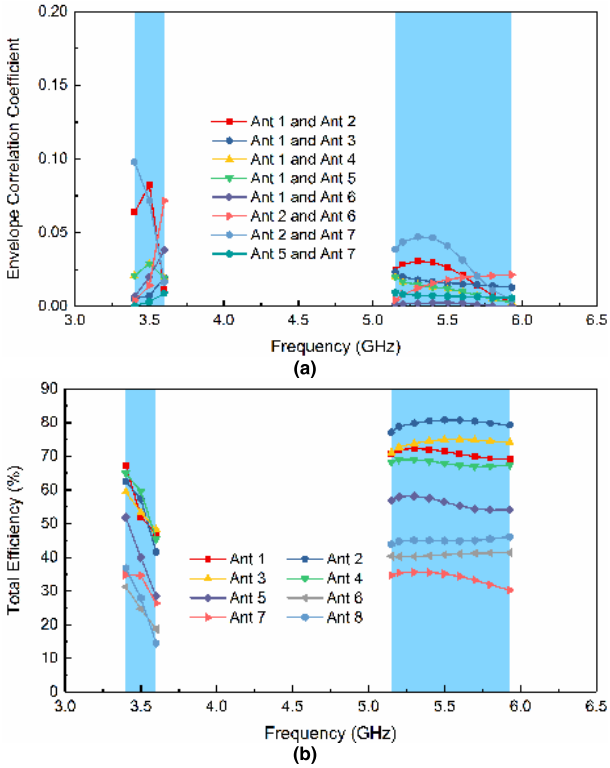

FIGURE 9. Simulated results of the proposed MIMO antenna array with single hand. (a) ECC. (b) Total efficiency.

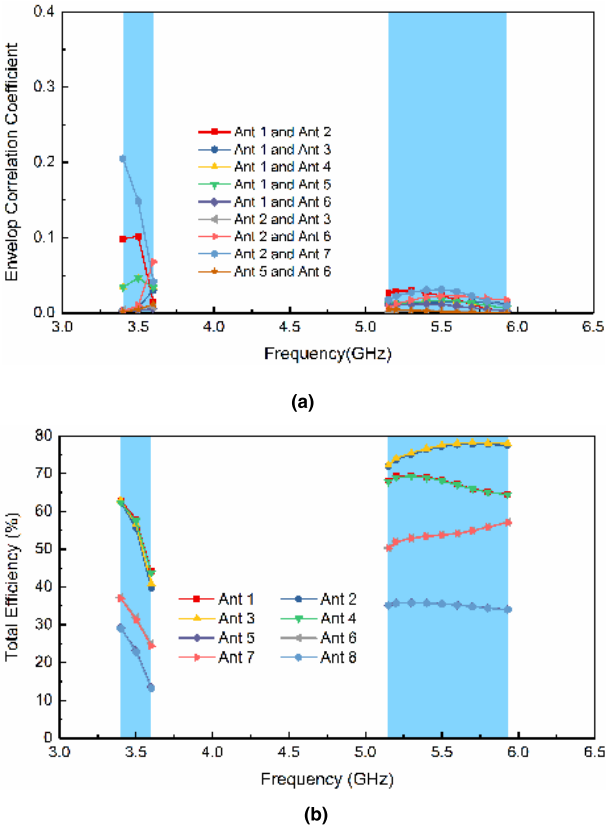

FIGURE 10. Simulated results of the proposed MIMO antenna array with two hands. (a) ECC. (b) Total efficiency.

hands on the antenna array need to be investigated. Therefore, the performance of the 8-antenna MIMO array in the presence of single hand, two hands, and SAM head have been analyzed and discussed, as illustrated in Figure 8.

At the single hand condition, i.e. the screen is positioned vertically, the involved simulated utility scenario is shown in Figure 8(a). As shown in Figure 9(a), the ECCs (ρ_{12} and ρ_{27}) increase within the LTE band 42, but still keep less than 0.1. Although the value is larger than that without the hand, it is rather small and acceptable. Yet, the total efficiencies of Ant 6 and Ant 8 close to the hand are reduced to 18%, which are nearly unusable at the LTE band 42. Hence, just as shown in Figure 9(b), the 8-antenna MIMO array is equivalent to a 6-antenna MIMO array applicable for 5G communications as well.

Furthermore, as shown in Figure 8(b), the screen is placed horizontally. At the two hands condition, Figure 10(a) shows that the ECCs (ρ_{12} and ρ_{27}) increase within the 3500-MHz band, and they are kept less than 0.2 and usable for mobile communication systems. By observing Figure 10(b) closely, the minimum total efficiencies of Ant 5 and Ant 8 close to the human hands are reduced to 13% at the 3500-MHz band, while other antennas can still work well with acceptable total efficiencies greater than 26%. Hence, at the reading condition, the designed 8×8 MIMO antenna array is equivalent to a 6×6 antenna array.

Figure 8(c) presents the involved simulated utility scenario in the presence of the SAM head and single hand. Figure 11 plots the simulated ECC and total efficiency. It can be found that the ECCs increase within the two frequency bands, but maintain less than 0.3. Though larger than those of the above two utility scenarios, the ECC remains lower than 0.5 and acceptable. As presented in Figure 11(b), Ant i ($i = 1, 2, 3, 4$) can work well with the total efficiency of higher than 20% approximately within the two frequency bands. However, the total efficiencies of Ant i ($i = 5, 6, 7, 8$) close to the SAM head and hand diminish to 14%, which are almost unusable at the LTE band 42. Thus, the designed 8×8 MIMO antenna array is equivalent to a 4×4 MIMO antenna array, which can still be applied for 5G communications.

E. EFFECTS OF DISPLAY PANEL

Figure 12 shows the simulated S-parameters of the 8-antenna MIMO array with and without a common display screen. As the structure of the designed antenna array is symmetric, only the simulated results of Ant 1 and Ant 2 are given. As shown in Figure 12, the display panel is mounted on a grass ($\varepsilon_r = 5.5$) substrate with a size of 124 mm $\times$ 62 mm $\times$ 1 mm. It can be observed that there is a minor frequency shifting due to the existence of the display screen. However, we can still obtain a return loss of greater than 10 dB across the desired two frequency bands.

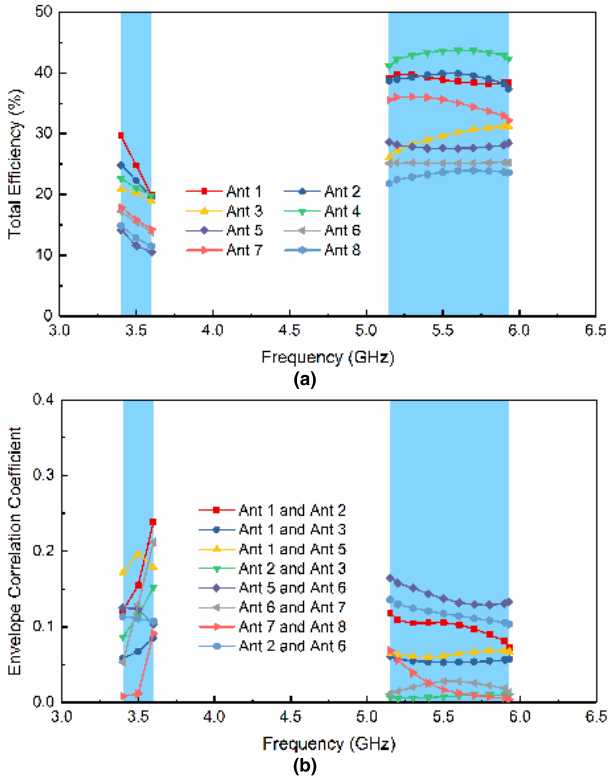

FIGURE 11. Simulated results of the proposed MIMO antenna array with SAM head and single head. (a) ECC. (b) Total efficiency.

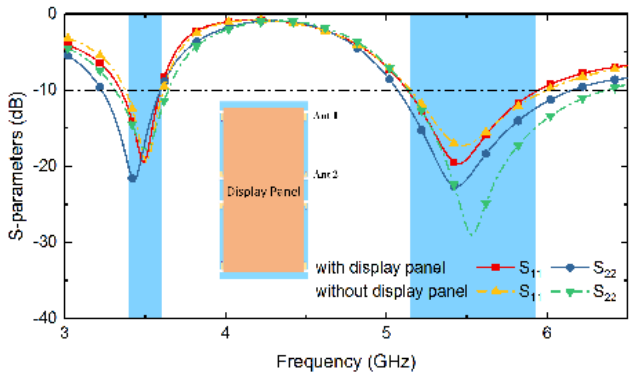

FIGURE 12. Simulated return loss of Ant1 and Ant2 with and without the display panel.

IV. EXPERIMENTAL RESULTS AND DISCUSSION

The manufactured 8-antenna MIMO array is given in Figure 13. The microstrip feed lines mounted on the top side of the substrate are shorted to the ground plane through vias. The *S*-parameters and farfield radiation patterns of each antenna element are measured in a microwave anechoic chamber.

Figure 14 compares the simulated and experimental return loss. Only those of Ant 1 and Ant 2 are given on account of the symmetric structure of the 8-antenna MIMO array. There exists subtle differences between the measured and simulated results because of the fabrication errors, SMA welding issues and environment effects. However, the measured results still have a good agreement with the simulated results. Compared

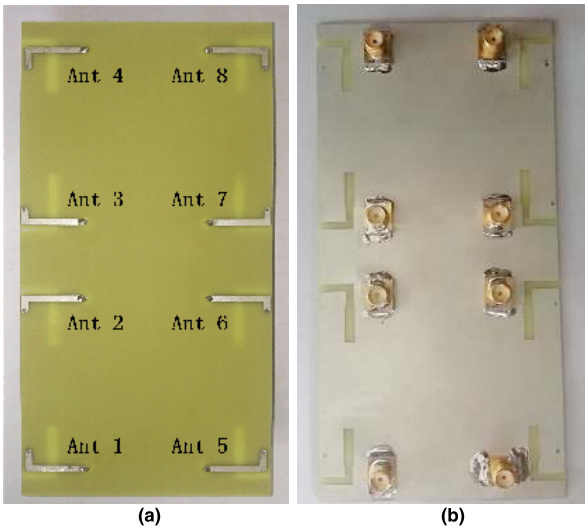

FIGURE 13. Prototype of the manufactured dual-band 8-antenna MIMO array. (a) Top view. (b) Bottom view.

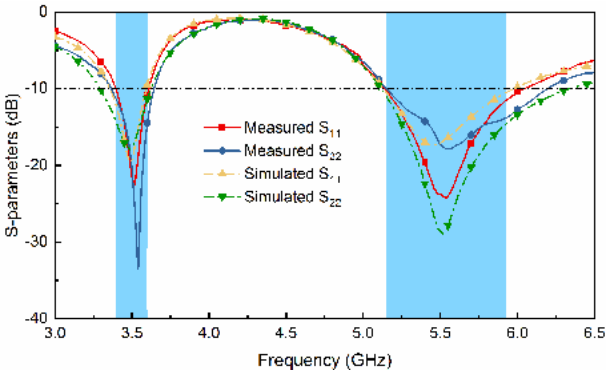

FIGURE 14. Simulated and experimental return loss of Ant1 and Ant2.

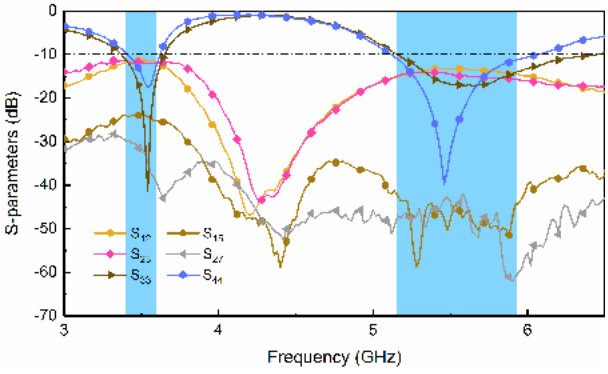

FIGURE 15. Experimental *S*-parameters of the manufactured MIMO antenna array.

with the simulated results, the performance of Ant 1 becomes slightly better within the LTE band 46. The measured 10-dB impedance bands are 220 MHz ranging from 3390 MHz to 3610 MHz and 920 MHz ranging from 5120 MHz to 6040 MHz.

The other experimental representative *S*-parameters of the manufactured 8-antenna MIMO array are given in Figure 15. Because of the structural symmetry, only the measured return

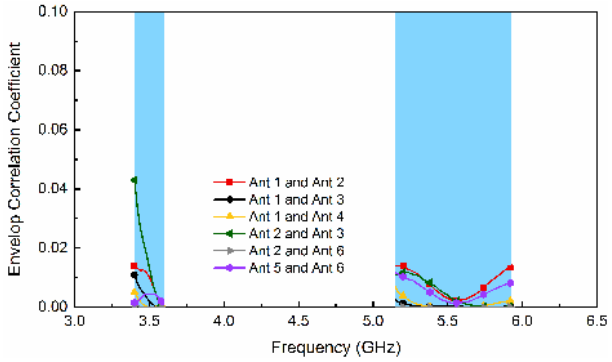

FIGURE 16. Experimental ECC results of the MIMO antenna array.

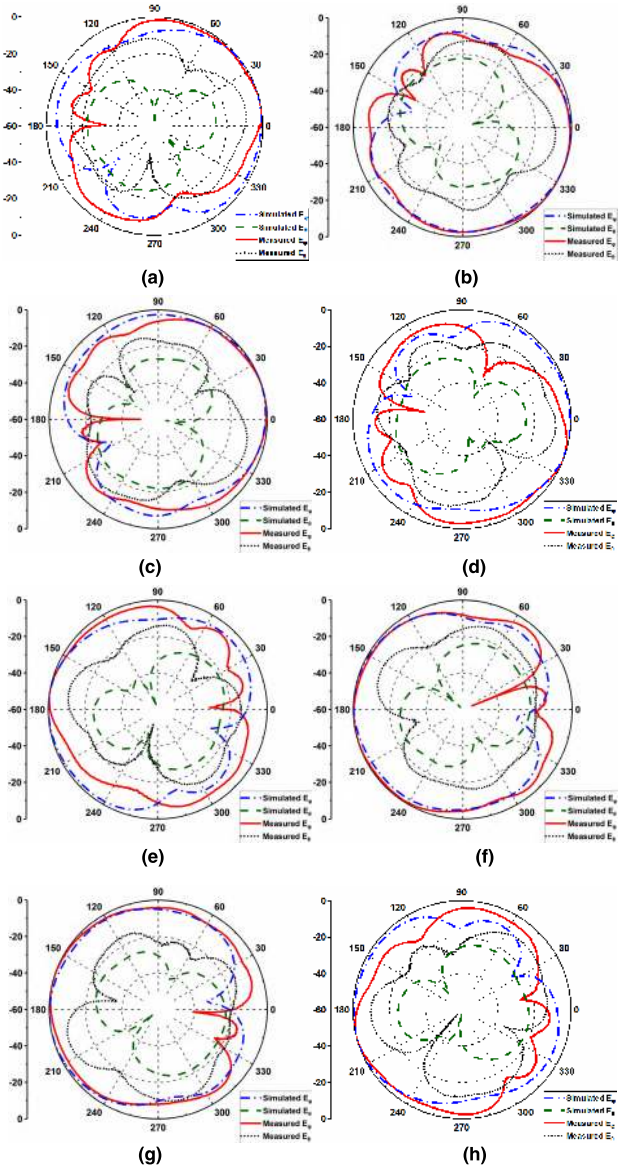

FIGURE 17. Normalized simulated and experimental farfield patterns at 3500 MHz in the x–y plane. (a) Ant1. (b) Ant 2. (c) Ant 3. (d) Ant 4. (e) Ant 5. (f) Ant 6. (g) Ant 7. (h) Ant 8.

loss of Ant i ($i = 3,\ 4$) are given. It shows that Ant 3 has a 10-dB impedance bandwidths of 7.4% (3380–3640 MHz) and

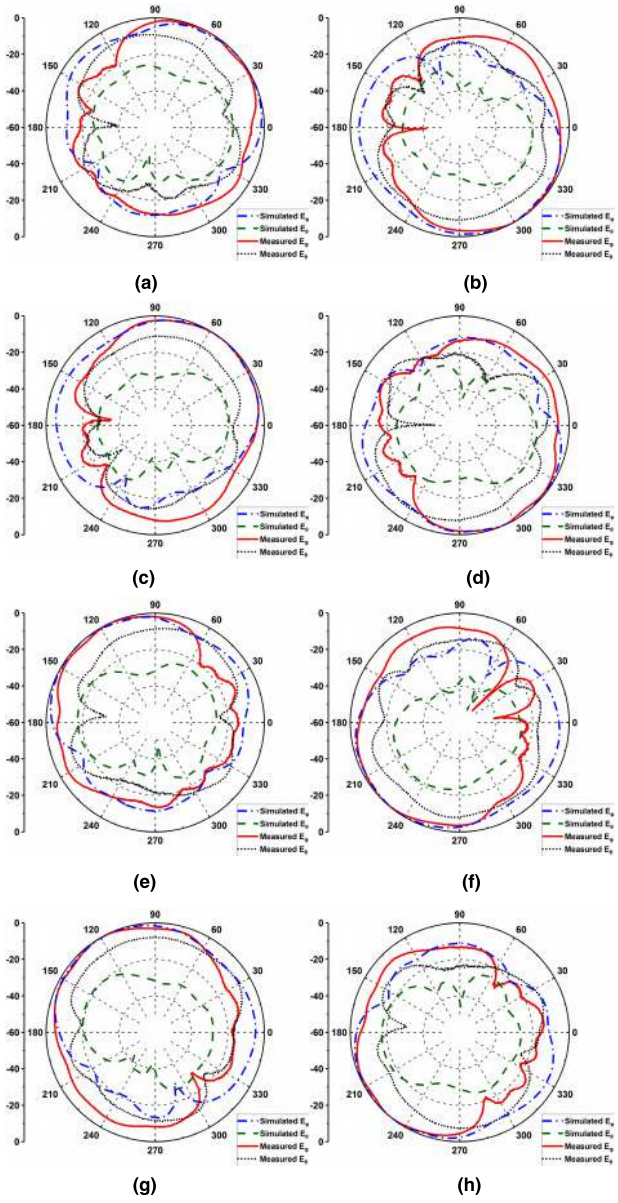

FIGURE 18. Normalized simulated and experimental farfield patterns 5500 MHz in the x–y plane. (a) Ant1. (b) Ant 2. (c) Ant 3. (d) Ant 4. (e) Ant 5. (f) Ant 6. (g) Ant 7. (h) Ant 8.

23.6% (5140–6440 MHz), and those of Ant 4 are 6.3% (3400 –3620 MHz) and 17.4% (5120–6080 MHz). Compared with the simulations, the experimental isolation (S_{12} and S_{23}) are relatively larger but better than 11.2 dB. In consistent with the simulations, the measured isolation between neighboring antennas on the narrow side, i.e. S_{15}, is relatively smaller that is greater than 23 dB within the 3500-MHz band and 5500-MHz band.

Using (2), the ECCs between arbitrary antenna elements are calculated, as depicted in Figure 16. The ECC is less than 0.1 within both frequency bands, validating that the proposed MIMO antenna array has good diversity performance.

The simulated and measured normalized farfield radiation patterns in the x-y plane are presented in Figures 17 and 18,

TABLE 2. Performance comparison between the proposed MIMO antenna array and reported ones.

Ref.	Bandwidth (MHz)	Dimensions (mm^3)	Isolation (dB)	ECC	No. of Ants.	Total Efficiency (%)
Proposed	3400—3600 5150—5925	140 × 70 × 1	≥11.2	≤0.08	8	51—59 (lower band) 62—80 (upper band)
[3]	3400—3800	150 × 75 × 0.8	NG	≤0.5	8 and 16	30–52 (8 × 8) 30–52 (16 × 16)
[4]	3400—3600	150 × 75 × 0.8	≥12.5	≤0.2	12	55-70
[6]	3400—3600 5150—5925	150 × 75 × 0.8	≥12	≤0.1 (lower band) ≤0.04 (upper band)	8	50–56 (lower band) 53–65 (upper band)
[7]	3400—3800 5150—5925	150 × 80 × 0.8	≥12	≤0.15 (lower band) ≤0.1 (upper band)	8 (lower band) 6 (upper band)	41–82 (lower band) 47–79 (upper band)
[9]	3400—3800 5150—5925	150 × 80 × 0.8	≥11	≤0.15 (lower band) ≤0.05 (upper band)	10	42–65 (lower band) 62–82 (upper band)

respectively, at 3500 MHz and 5500 MHz. Apart from the antenna element under test, all others are connected to 50 Ω matched loads. It can be observed that the measured results achieve a good agreement with the simulated ones. Besides, it can be concluded that the measured E_φ (co-polarization) is 9 dB larger than E_θ (cross polarization) in the main E-plane. Therefore, the antenna elements can achieve a relatively pure horizontal polarization. In detail, the Ant i ($i = 1, 2, 3, 4$) mainly radiates towards the +x direction at 3500 MHz, while the maximum radiation direction of the others is generally in the -x direction. Similar radiation patterns can also be found at 5500 MHz. Therefore, the proposed MIMO antenna array exhibits a good omnidirectional property, demonstrating the feasibility for 5G mobile terminal applications.

Table II summarizes the performance comparison between the proposed MIMO antenna array and the previous reported ones. When compared with those in [3] and [4], the proposed 8-antenna MIMO array is able to cover both LTE band 42 and LTE band 46. In addition, the proposed MIMO antenna array has the lowest ECC. It also owns the best impedance matching with a return loss of larger than 10 dB across the entire desired frequency bands. Furthermore, the proposed MIMO antenna array has higher total efficiencies. Therefore, the proposed MIMO antenna array generally outperforms the reported ones.

V. CONCLUSION

This paper investigates thoroughly a dual-band eight-antenna array based on slot SIRs for future 5G MIMO applications. It realizes a return loss of higher than 10 dB, an inter-element isolation of greater than 11.2 dB, an ECC of lower than 0.1, and a total efficiency of more than 51% within the LTE band 42 and LTE band 46 for each antenna element. The measured results well agree with the simulations. The channel capacity is expected to be as high as 36.9–37.9 bps/Hz and 38.5–40.9 bps/Hz within the two frequency bands, respectively. A low ECC and good MIMO performance also can be maintained in the presence of the SAM head and human hands. Hence, the proposed 8 × 8 MIMO antenna array can be a promising candidate for 5G multiband MIMO applications in mobile terminals.

REFERENCES

[1] H. Li, Z. T. Miers, and B. K. Lau, "Design of orthogonal MIMO handset antennas based on characteristic mode manipulation at frequency bands below 1 GHz," *IEEE Trans. Antennas Propag.*, vol. 62, no. 5, pp. 2756–2766, May 2014.

[2] H. Elshaer, M. N. Kulkarni, F. Boccardi, J. G. Andrews, and M. Dohler, "Downlink and uplink cell association with traditional macrocells and millimeter wave small cells," *IEEE Trans. Wireless Commun.*, vol. 15, no. 9, pp. 6244–6258, Sep. 2016.

[3] K. L. Wong, J.-Y. Lu, L.-Y. Chen, W.-Y. Li, and Y.-L. Ban, "8-antenna and 16-antenna arrays using the quad-antenna linear array as a building block for the 3.5-GHz LTE MIMO operation in the smartphone," *Microw. Opt. Technol. Lett.*, vol. 58, no. 1, pp. 174–181, Jan. 2016.

[4] M.-Y. Li, Y.-L. Ban, Z.-Q. Xu, J. Guo, and Z.-F. Yu, "Tri-polarized 12-antenna MIMO array for future 5G smartphone applications," *IEEE Access*, vol. 6, pp. 6160–6170, 2018.

[5] H. Xu *et al.*, "A compact and low-profile loop antenna with six resonant modes for LTE smartphone," *IEEE Trans. Antennas Propag.*, vol. 64, no. 9, pp. 3743–3751, Sep. 2016.

[6] H. Zou, Y. X. Li, C.-Y.-D. Sim, and G. L. Yang, "Design of 8 × 8 dual-band MIMO antenna array for 5G smartphone applications," *Int. J. RF Microw. Comput.-Aided Eng.*, vol. 28, Nov. 2018, Art. no. e21420.

[7] Y. X. Li, C.-Y.-D. Sim, Y. Luo, and G. L. Yang, "12-port 5G massive MIMO antenna array in sub-6 GHz mobile handset for LTE bands 42/43/46 applications," *IEEE Access*, vol. 6, pp. 344–354, 2018.

[8] Y.-L. Ban, C. Li, C.-Y.-D. Sim, G. Wu, and K.-L. Wong, "4G/5G multiple antennas for future multi-mode smartphone applications," *IEEE Access*, vol. 4, pp. 2981–2988, 2016.

[9] Y. X. Li, C.-Y.-D. Sim, Y. Luo, and G. L. Yang, "Multiband 10-antenna array for sub-6 GHz MIMO applications in 5-G smartphones," *IEEE Access*, vol. 6, pp. 28041–28053, 2018.

[10] D. Q. Liu, M. Zhang, H. J. Luo, H. L. Wen, and J. Wang, "Dual-band platform-free PIFA for 5G MIMO application of mobile devices," *IEEE Trans. Antennas Propag.*, vol. 66, no. 11, pp. 6328–6333, Nov. 2018.

[11] J. L. Guo, L. Cui, C. Li, and B. H. Sun, "Side-edge frame printed eight-port dual-band antenna array for 5G smartphone applications," *IEEE Trans. Antennas Propag.*, vol. 66, no. 12, pp. 7412–7417, Dec. 2018.

[12] S. Zhang, K. Zhao, Z. Ying, and S. He, "Adaptive quad-element multi-wideband antenna array for user-effective LTE MIMO mobile terminals," *IEEE Trans. Antennas Propag.*, vol. 61, no. 8, pp. 4275–4283, Aug. 2013.

[13] S.-W. Chen, D.-Y. Wang, and W.-H. Tu, "Dual-band/tri-band/broadband CPW-fed stepped-impedance slot dipole antennas," *IEEE Trans. Antennas Propag.*, vol. 62, no. 1, pp. 485–490, Jan. 2014.

[14] S. Blanch, J. Romeu, and I. Corbella, "Exact representation of antenna system diversity performance from input parameter description," *Electron. Lett.*, vol. 39, no. 9, pp. 705–707, May 2003.
[15] J. X. Li, Y. S. Jiang, A. X. Zhang, J. Chen, and X. Sheng, "Design of a compact multiband internal antenna for mobile application," *Microw. Opt. Technol. Lett.*, vol. 53, no. 12, pp. 2865–2868, 2011.
[16] R. G. Vaughan and J. B. Andersen, "Antenna diversity in mobile communications," *IEEE Trans. Veh. Technol.*, vol. VT-36, no. 4, pp. 149–172, Nov. 1987.
[17] S. Pahadsingh and S. Sahu, "Four port MIMO integrated antenna system with DRA for cognitive radio platforms," *Int. J. Electron. Commun.*, vol. 92, pp. 98–110, May 2018.
[18] L. Zheng and D. N. C. Tse, "Diversity and multiplexing: A fundamental tradeoff in multiple-antenna channels," *IEEE Trans. Inf. Theory*, vol. 49, no. 5, pp. 1073–1096, May 2003.
[19] R. Tian, B. K. Lau, and Z. Ying, "Multiplexing efficiency of MIMO antennas," *IEEE Antennas Wireless Propag. Lett.*, vol. 10, pp. 183–186, 2011.

JIANXING LI (S'15–M'18) received the B.S., M.S., and Ph.D. degrees in electromagnetic field and microwave technology from Xi'an Jiaotong University, Xi'an, China, in 2008, 2011, and 2016, respectively.

From 2014 to 2016, he was a Visiting Researcher with the Department of Electrical and Computer Engineering, Duke University, Durham, NC, USA, under the financial support from the China Scholarship Council. He is currently a Lecturer with the School of Electronic and Information Engineering, Xi'an Jiaotong University. His current research interests include antennas, microwave and millimeter-wave circuits, and metamaterials. He serves as a Reviewer for several international journals, including the IEEE Access, *IET Electronics Letters*, the *International Journal of RF and Microwave Computer-Aided Engineering*, and the *International Journal of Electronics and Communications*.

XIAOKE ZHANG received the B.S. degree in information engineering from Xi'an Jiaotong University, Xi'an, China, in 2017, where she is currently pursuing the M.S. degree in electronic and communication engineering with the Electromagnetics and Communication Laboratory. Her current research interests include multiple-input and multiple-output (MIMO) antenna arrays, and millimeter-wave antennas.

ZHI WANG received the Ph.D. degree in computer science from Xi'an Jiaotong University, Xi'an, China, in 2014, where he is currently a Lecturer with the School of Software Engineering. His research interests include mobile communications, wireless networks, smart sensing, and mobile computing.

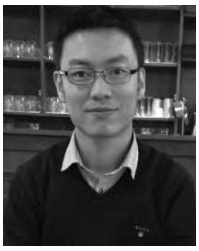

XIAOMING CHEN received the B.Sc. degree in electrical engineering from Northwestern Polytechnical University, Xi'an, China, in 2006, and the M.Sc. and Ph.D. degrees in electrical engineering from the Chalmers University of Technology, Gothenburg, Sweden, in 2007 and 2012, respectively.

From 2013 to 2014, he was a Postdoctoral Researcher with the Chalmers University of Technology. From 2014 to 2017, he was with Qamcom Research and Technology AB, Gothenburg. Since 2017, he has been a Professor with Xi'an Jiaotong University, Xi'an. His research areas include multiple-input and multiple-output (MIMO) antennas, over-the-air (OTA) testing, reverberation chambers, and hardware impairments and mitigation.

Dr. Chen was a recipient of the Outstanding AE Award, in 2018, and the International Union of Radio Science (URSI) Young Scientist Awards, in 2017 and 2018. He serves as an Associate Editor (AE) for the journal of IEEE Antennas and Wireless Propagation Letters. He was also a Guest Editor of the Special Issue on Metrology for 5G Technologies in the journal of *IET Microwaves, Antennas and Propagation*.

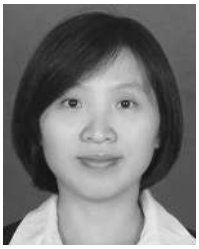

JUAN CHEN (M'18) received the Ph.D. degree in electromagnetic field and microwave technology from Xi'an Jiaotong University, Xi'an, China, in 2008.

From 2016 to 2017, she was a Visiting Researcher with the Department of Electrical and Computer Engineering, Duke University, Durham, NC, USA, under the financial support from the China Scholarship Council. She is currently a Professor with the Shenzhen Research School, Xi'an Jiaotong University, and also with the School of Electronic and Information Engineering, Xi'an Jiaotong University. Her current research interests include numerical electromagnetic methods, advanced antenna designs, and graphene theory and application.

YINGSONG LI (M'14) received the B.S. degree in electrical and information engineering and the M.S. degree in electromagnetic field and microwave technology from Harbin Engineering University, Harbin, China, in 2006 and 2011, respectively, and the Ph.D. degree from the Kochi University of Technology (KUT), Japan, and Harbin Engineering University, in 2014.

He was a Visiting Scholar with the University of California, Davis, from 2016 to 2017, and also with the University of York, U.K., in 2018. He has been a Full Professor with Harbin Engineering University, since 2014. He is currently a Visiting Professor with Far Eastern Federal University (FEFU) and KUT. His current research interests include remote sensing, underwater communications, signal processing, radar, SAR imaging, compressed sensing, and antennas.

Dr. Li is a Senior Member of the Chinese Institute of Electronics (CIE). He is an Associate Editor of the IEEE Access and the *Applied Computational Electromagnetics Society Journal*. He is an Area Editor of the *AEÜ-International Journal of Electronics and Communications*. He also serves as a Reviewer for more than 20 journals.

ANXUE ZHANG received the B.S. degree in electrical and electronics engineering from Henan Normal University, Xinxiang, China, in 1996, and the M.S. and Ph.D. degrees in electromagnetic fields and microwave technology from Xi'an Jiaotong University, Xi'an, China, in 1999 and 2003, respectively.

He is currently a Professor with the School of Electronic and Information Engineering, Xi'an Jiaotong University. His current research interests include antennas and electromagnetic wave propagation, RF and microwave circuit design, array signal processing, and metamaterials.